Comparative Diagnostic Studies on Marek's Disease in chickens by Use of Histopathology and Molecular Investigation

Abdel Moniem A Ali, El-Sayed RA El-Attar, Mohamed H Mohamed and Heba M Abdel Ghany

Pathology Dept, Faculty of Vet Medicine, Zagazig University, Egypt.

ABSTRACT

Hundred-twenty five diseased or freshly dead birds from different domestic poultry flocks chickens flocks layers breeds as (lohman, novagen and native breed as sasso) and sporadic cases were collected and necropsied between the period from Aug. 15, 2012 to Nov. 8, 2014 and samples from each case were collected. The collecting samples were subjected to the pathology and some selected ones (7) for PCR laboratory (stored freezing -20ºC). Liver, spleen, heart, lungs, kidneys, intestine, ovary, proventriculus, gizzard, skin, nerve, bursa of Fabricius, eye and brain were the main examined organs.

Nervous disorders were observed with gasping, diarrhea and emaciation were also visualized besides up to 15% mortalities. Enlargement of sciatic nerves, irregular pupil, grayish-white nodules in the visceral organs and focal discolored areas on the skin were noticed besides ovarian congestion and misshaped ova. Microscopically, heavy pleomorphic cellular infiltrations of small lymphocytes, lymphoblasts, plasma cells and few mesenchymal cells proliferation and heterophil infiltration were seen in all examined organs. Extensive tissue necrosis, congestion, hemorrhage and edema were associated the infiltrations. Six-out of seven were PCR positive for Marek's disease virus

All investigated birds were regarded as one disease with lesions possessing the same characteristics, but of varying severity (by histopathology). PCR was best tool to detect and confirm the Marek's disease virus; but consuming time.

INTRODUCTION

Marek's disease (MD) is a lymphoproliferative disease induced by the alpha-herpesvirus Marek's disease virus (MDV) or Gallid herpesvirus 2 (GaHV-2). MDV has evolved towards more virulent forms in the recent decades. The efficacy of MDV vaccines has decreased concomitantly with the increase in virulence of field isolates. The disease was a major disease problem and source of great economic losses in poultry *(1)*. The disease is characterized by the presence of T cell lymphoma as well as infiltration of nerves, skin, eye and visceral organs by lymphocytes *(2)*.

MDV is an airborne pathogen with infection occurring via inhalation *(3-5)*. Virus shedding occurs by infected feather follicle epithelium *(6,7)*. The resulting dust and dander from dead stratified cells and moulted feathers can then remain in the environment and act as a reservoir for chicken infection. Clinical signs are varied and result in significant morbidity and mortality depending on host genetic susceptibility and virulence of the MDV strain *(8)*. Symptoms include polyneuritis (an enlargement of multiple peripheral nerves), visceral lymphoma (tumors affecting organs such as the heart, liver, spleen etc.), acute transient paralysis, immunosuppression, brain edema and acute rash *(9, 10)*. There has been a change in the types of clinical signs since the disease was first noted when chronic polyneuritis was the only sign. Since then, the

list of clinical signs described above expanded gradually over the decades *(11)*.

The primary diagnosis of avian oncogenic viruses is based on the gross and microscopic lesions, and conventional PCR besides the history and clinical signs. Grossly, the disease is characterized by paralysis of legs, wings and neck, and tumor nodules in visceral organs depending upon the tissue or organ involved. Gray eye (iris) or irregular pupil, vision impairment, blindness, skin lesions and immunosuppression were observed, however, the microscopic lesions were represented by mononuclear cell infiltrations in one or more of the following tissues; peripheral nerves, gonads, lymphoid organs, iris, muscles, skin and other visceral organs *(12)*.

PCR appears to be the method of choice for the diagnosis of avian oncogenic viruses because it overcomes many of the challenges encountered in the differential diagnosis and enables the detection of multiple viral infections *(13)*.

The present study was carried out to confirm that the histopathology is still rapid diagnostic tool with conventional diagnostic PCR technique. Prevalence, clinical signs and postmortem lesions were the first observations to exclude Marek's-diseased birds.

MATERIALS AND METHODS

Collection of tissue specimens

Hundred-twenty five diseased or freshly dead birds from different domestic poultry flocks and sporadic cases were collected and necropsied between the period from Aug. 15, 2012 to Nov. 8, 2014. Samples from each case were collected. The collecting samples were subjected to the pathology and some selected ones (7) to the PCR laboratory (stored freezing -20°C). Liver, spleen, heart, lungs, kidneys, intestine, ovary, proventriculus, gizzard, skin, nerve, bursa, eye and brain were the main examined organs.

Diagnosis of Marek's disease

Diagnosis of MD was performed on the basis of clinical signs, postmortem lesions, histopathology and PCR investigation.

Pathological examination

The necropsy was performed for detection of tumors in various tissues and visceral organs. Specimens were collected from such tissues collected and fixed in 10% buffered neutral formalin solution, dehydrated in gradual ethanol (70-100%), cleared in xylene, and embedded in paraffin. Five-micron thickness paraffin sections were prepared and then routinely stained with hematoxylin and eosin (**HE**) dyes *(14)* and then examined microscopically.

PCR technique

Extraction of DNA *(15)*:

According to ABIOpure Genomic DNA extraction kit instructions

200 µl of GB Buffer was added to 200 µl of the sample into the 1.5 ml microcentrifuge tube and mixed by vortex and then Incubated at room temperature for 10 minutes or until the sample lysate is clear.

At this time, the required Elution Buffer was preheated in a 70°C water bath.200 µl of absolute ethanol was added to the sample lysate and vortexed immediately for 10 seconds. GD Column was placed in a 2 ml Collection Tube and the mixture was transferred to the GD Column and then centrifugated at 14000 rpm for 3 minutes. The 2 ml Collection Tube containing the flow-through was discarded and the GD Column was placed in a new 2 ml Collection Tube.400 µl of W1 Buffer was added to the GD Column and then centrifugated at 14000 rpm for 30 seconds. The flow-through was discarded and the GD Column was placed back in the 2 ml Collection Tube.600 µl of Wash Buffer (ethanol added) was added to the GD Colum and then centrifuge at 14000 rpm for 3 minutes. The flow-through was discarded and the GD Column was placed into a clean 1.5 ml microfuge tube. The dried GD Column was

transferred into a clean 1.5 ml microfuge tube and 100 µl of preheated Elution Buffer was added to the center of the column matrix. It was Let stand for 3 minutes and then centrifugated at 14000 rpm for 30 seconds to elute the purified DNA.

Oligonucleotide primers used in cPCR

They have specific sequence and amplify a specific product as shown in Table (1).

Table 1. Oligonucleotide primers sequences

Source: **Metabion (Germany).**

Virus	Gene	Primer/ probe sequence 5'-3'	Amplified Segment (bp)	References
MD	ICP4	MDV-1.1 GGATCGCCCACC ACGATTACTACC MDV-1.8 ACTGCCTCACAC AACCTCATCTCC	247	*16*
REV	Env	REV-env-F ATG AAG ACG GGC CTA A REV-env-R AAA GGG GAG GCT AAG A	402	*17*
ALV-A	Env	H5-F GGATGAGGTGACTAAGAAAG EnvA-R AGAGAAAGAGGGGYGTCTAAGGAGA	740	*18*

Table 2. Preparation of PCR Master Mix according to Emerald Amp GT PCR mastermix (Takara) Code No. RR310A kit

Component	Volume/reaction
Emerald Amp GT PCR mastermix (2x premix)	12.5 µl
PCR grade water	4.5 µl
Forward primer (20 pmol)	1 µl
Reverse primer (20 pmol)	1 µl
Template DNA	6 µl
Total	25 µl

Cycling conditions of the primers during cPCR:

Temperature and time conditions of the different primers during PCR are shown in Table (3) according to specific authors and Emerald Amp GT PCR mastermix (Takara) kit

Table 3. Cycling conditions of the different primers during cPCR

Virus	Primary Denaturation	Secondary Denaturation	Annealing	Extension	Final Extension	No. of cycles	References
MD	95°C 10 min.	94°C 30 sec.	58°C 45 sec.	72°C 45 sec.	72°C 10 min.	35	*(16)*
REV	95°C 10 min.	94°C 15 sec.	50°C 45 sec.	72°C 45 sec.	72°C 10 min.	35	*(19)*
ALV-A	95°C 15 min.	94°C 1 min.	55°C 1 min.	72°C 1 min.	72°C 10 min.	35	*(18)*

DNA Molecular weight marker:

The ladder was mixed gently by pipetting up and down. 6 µl of the required ladder were directly loaded.

Agarose gel electrophoreses with modification

Electrophoresis grade agarose (1.5 g) was prepared in 100 ml TBE buffer in a sterile flask, it was heated in microwave to dissolve all granules with agitation, and allowed to cool at 70°C, then 0.5µg/ml ethedium bromide was added and mixed thoroughly. The warm agarose was poured directly in gel casting apparatus with desired comb in apposition and left at room temperature for polymerization.

The comb was then removed, and the electrophoresis tank filled with TBE buffer. Ten to fifteen µl of each PCR product samples, negative control and positive control were loaded to the gel. The power supply was 1-5 volts/cm of the tank length. The run was stopped after about 30 min and the gel was transferred to UV cabinet. The gel was photographed by a gel documentation system and the data was analyzed through computer software.

RESULTS

Incidence

Ninety-seven out of 125 (77.6%) examined tissues specimens were regarded as one disease entity with lesions possessing the same characteristics, but of varying severity. Such lesions were elucidated as Marek's disease which confirmed by PCR results.

Clinical Signs

The consistent clinical signs observed were whitish-yellow diarrhea and ruffled feathers firstly observed. Nervous disorders of the neck, wings or legs and one leg stretched foreward were observed. Gasping and emaciation were finally visualized besides up to 15% mortalities.

PCR Findings

Fig.1. illustrates the PCR results which showed 6-out of 7 were positive.

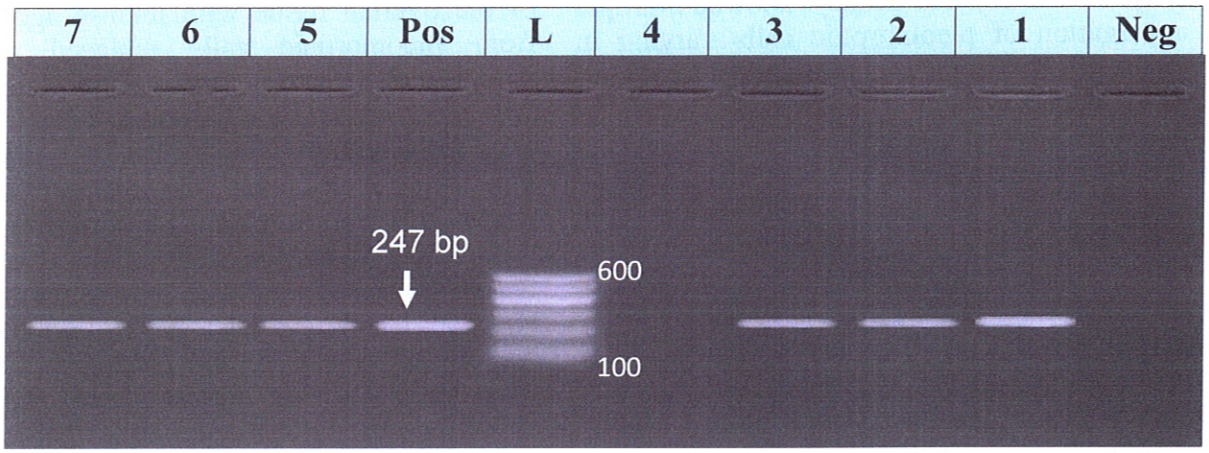

Pcr result: six liver samples were positive and one sample was negative of 7 sick chickens
L= marker pos= positive Neg= negative

Pathological Findings

Macroscopically, grayish-white or grayish-yellow nodules were seen scattered on the surface of most organs mainly liver, heart, spleen and kidneys (Fig 2 and 3). These organs were enlarged in sizes and friable in consistency. Enlargement and thickening of sciatic nerves (Fig 4), irregular pupil, and focal discolored areas on the skin were noticed besides ovarian congestion and misshaped ova had been observed. The brain of some cases showed severely congested meninges besides hemorrhagic patches.

Microscopically, the liver was focally or diffusely infiltrated with pleomorphic cellular aggregates of many small lymphocytes, lymphoblasts, plasma cells and few fibroblasts. These cells were firstly accumulated in the interlobular connective tissue especially around the small blood vessels (Fig 5). These foci were hyperplastic and spread by extension into the adjacent areas. They often fused together and form large masses of various sizes .These foci were rarely seen in the form of ill-defined nodular hyperplasia. Diffuse infiltration was partly seen in the hepatic parenchyma and perivascular sinusoids (Fig 6). Eosinophilic intranuclear inclusion bodies and numerous mitoses were visualized in some lymphoblasts (Fig 7 and 8). Extensive coagulative necroses were noticed in the contagious zone of cellular infiltrations. Huge numbers of heterophils were detected in the portal areas and intermingled the hepatic and the neoplastic cells. Severe congestion of hepatoportal blood vessels, hemorrhages and perivascular edema were also encountered besides some degenerative changes of hydropic type were detected. The spleen showed marked infiltration of the large cells with vesicular nuclei (lymphoblasts) around the splenic arteries which gradually spread into necrotic splenic parenchyma (Fig 9). In the more severe cases, the splenic parenchyma was distorted and completely replaced by these cells. Some heterophils and reticular cells were noticed besides congestion of the remaining blood vessels. The heart revealed irregular sized areas of pleomorphic aggregates replacing the myocardium .The latter showed focal atrophy, degeneration and necrosis with heterophilic infiltrations. Focal aggregations of the neoplastic cells were observed in the loose connective tissue of the subepicardial area and

the fat tissue around the coronary arteries. Sometimes, the cell accumulations were seen diffusely or focally among the muscle fibers (Figs 10 and 11). The kidneys showed multiple aggregation of pleomorphic cells varying in the extent between the renal tubules. The latter were severe necrotic and represented by pyknosis, karyorrhexis and karyolysis (Fig 12). In some cases, the proliferation was so extreme and the renal parenchyma was completely replaced by aforementioned cells (Fig13). Lymphoid cell infiltration was seen in and around the lamina propria of the ureter in almost every case. The lungs showed focal pleomorphic cells aggregates of mature lymphocytes, plasma cells and a fewly lymphoblasts particularly in the connective tissue and around the blood vessels in the interlobular septa (Fig 14). In more severe cases, the pulmonary tissue was completely replaced by a forementioned cells except the parabronchi. Sometimes, the lymphoid proliferation was seen in the wall of the secondary bronchi, inducing catarrhal bronchitis with perivascular aggregations of pleomorphic cells (Fig 15). Large areas of caseous necrosis were rarely seen in some cases. Pulmonary congestion, hemorrhage and edema were also visualized. The proventriculus showed invasion of the mucosa, muscularis mucosa, submucosa, lobules of the glands, muscular layers and subserosa by pleomorphic infiltration from lymphocyte, lymphoblast and heterophil cells (Fig 16). Extensive mucosal and glandular necroses with congestion of blood vessels were seen (Fig 17). The gizzard revealed pleomorphic cell aggregates around the small blood vessels in the submucosa, muscle layers and subserosa. Mucosal necrosis was also observed (Fig 18 and 19). The intestine showed replacement the all intestinal layers with pleomorphic aggregations with thickening of the intestinal wall (Figs 20 and 21). The bursa of Fabricius showed ill-defined lymphoid follicles with necrosis in the lymphoid cells at the center of the follicles. Sometimes, fibrous connective tissue proliferation was the cause of such demarcation. The tumor cells were seen in the interfollicular zones and rarely extended to the adjacent lymphoid follicles (Fig 22). The ovary showed focal replacement of the ovarian tissue with intense aggregates from pleomorphic cells replaced ovarian stroma. Such ova was degenerated or misshaped. Severe congestion and hemorrhage were seen around such infiltrations (Fig 23). The skeletal muscles showed perivascular tumor cell aggregations. Such aggregations were extended into the surrounding tissues. In severe cases, wide areas of muscle tissue were replaced by these cells. At the same time, hyaline degeneration and Zenker's necrosis were noticed in the muscle fibers. Muscular atrophy was occasionally seen particularly with cases showed paralysis. The skin showed hypertrophied feather follicles with compact lymphoid aggregates in the dermis particularly around the dermal blood vessels (Figs 24, 25 and 26). These aggregates were rarely seen at the subepidermal zone inducing atrophy of the epidermal cells and ulcerations. The reticular and papillary layers of the dermis were focally hyalinized and necrotic. The hypodermis was focally infiltrated with these cells. The sciatic nerve was focally thickened and showed demyelination and few pleomorphic cellular infiltrations. Edema and hyalinization of perineurium connective tissue were observed (Fig 27).The eye showed severe vacuolation and detached choroidal epithelium from the underlying sclera. Severe congestion and hemorrhage were noticed besides few round cells infiltrations. Sometimes, pale eosinophilic material between different layers was seen. The brain revealed vasogenic (in the ventricles and Virchow Robin spaces) and cytogenic (vacuolated neurons and neuronoglias) edema. Demyelination and encephalomalacia were visualized in the white matter (Fig 28). Numerous pleomorphic aggregations of T lymphocyte, plasma cells, heterophil cells the brain tissue (Fig 29).Such cells were focally replaced the brain tissue. Congestion and extensive hemorrhage were also reported besides degenerated neurons, satellitosis and neuronophagia.

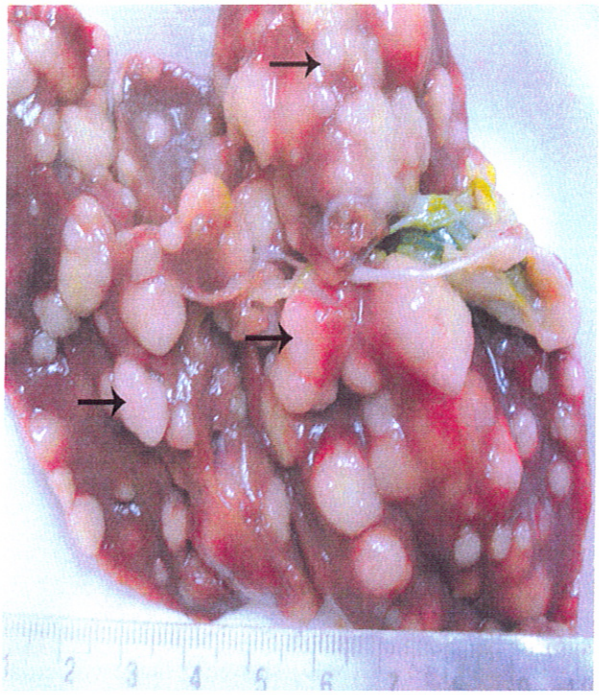

Fig 2. Liver of (MD) showing grayish-white or grayish-yellow nodules of variable sizes on it's surface.

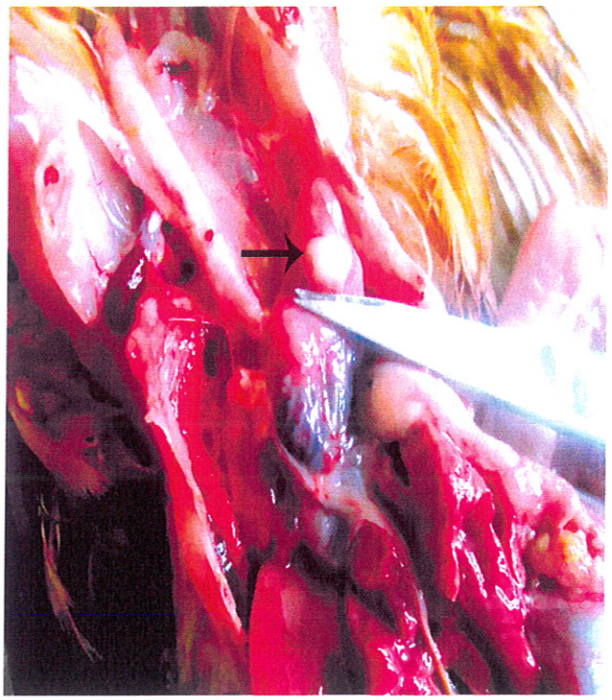

Fig 3. Heart of (MD) showing large white elevated nodule.

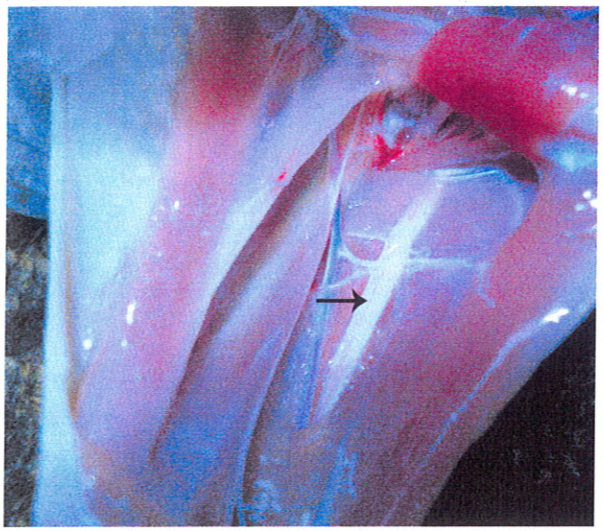

Fig 4. Sciatic nerve of (MD) showing mild enlargement and thickening.

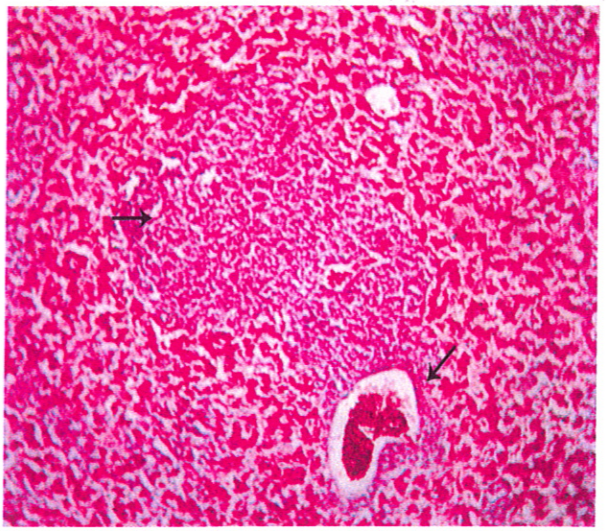

Fig.5. Liver showing multiple interstitial and perivascular pleomorphic aggregates of small lymphocytes, lymphoblasts, plasma cells and few fibroblasts (arrow), HE X100.

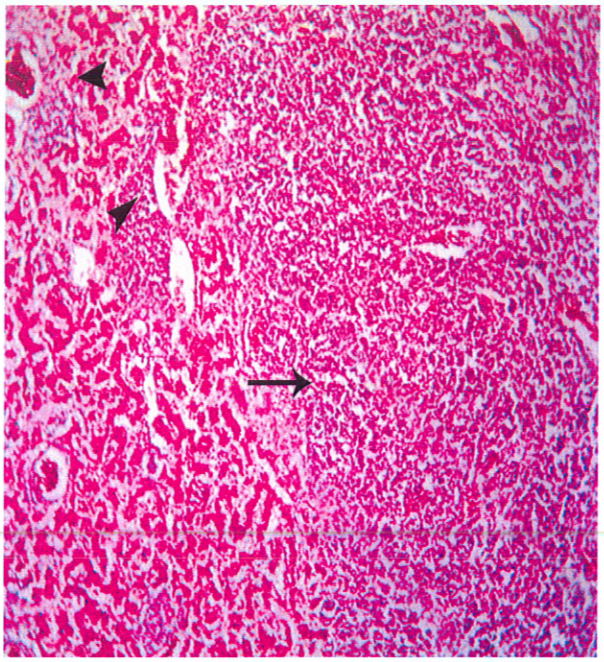

Fig.6.Liver of (MD) showing diffuse replacement of hepatic parenchyma by pleomorphic aggregation of small lymphocytes, lymphoblast, plasma cells and few fibroblasts (arrow) mainly perivascular (arrow head), HEX100.

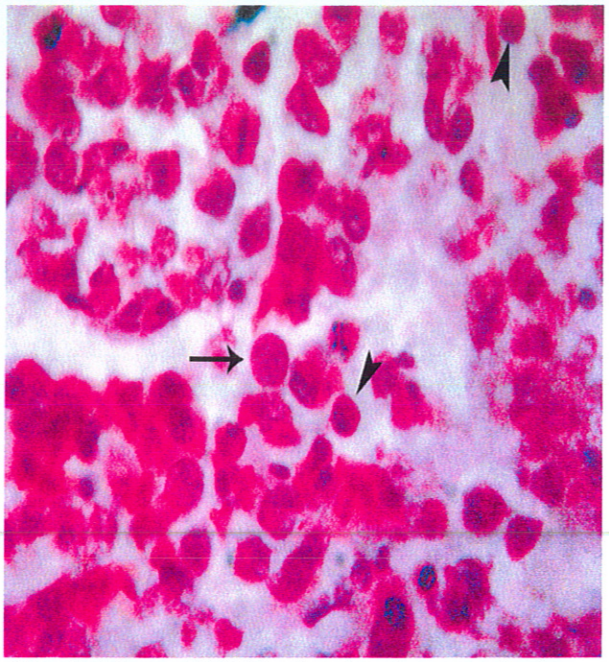

Fig. 7. Liver of (MD) showing large vesicular hyperchromatic nuclei with abundant esinophilic cytoplasm (arrow) and numerous mitotic figures (arrow head), HEX1000.

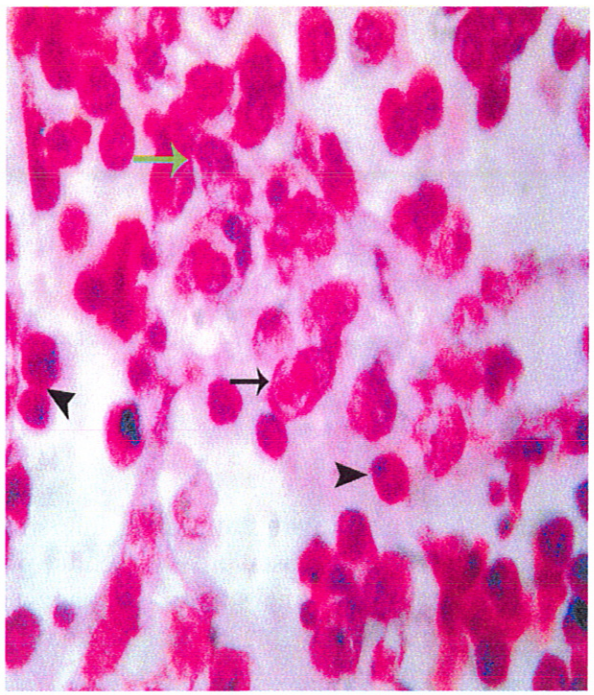

Fig.8. Liver of (MD) showing eosinophilic intranuclear inclusion bodies (arrow) with large vesicular hyperchromatic nuclei (arrow head) and mitoses were visualized in some lymphoblasts (green arrow), HEX1000.

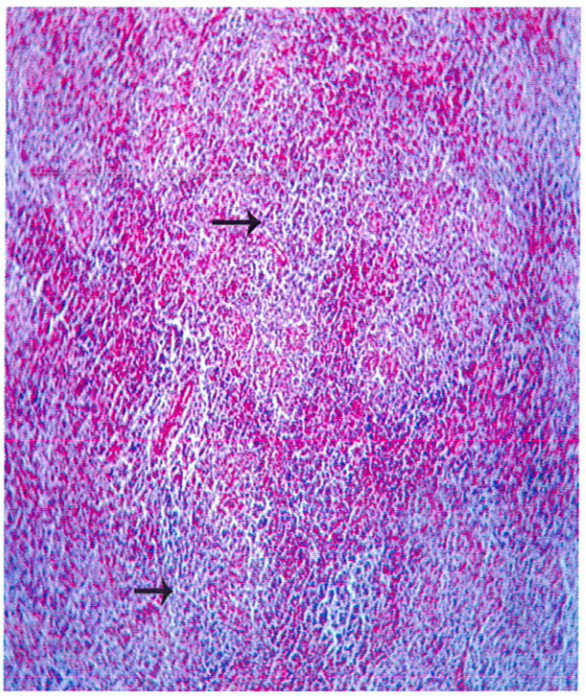

Fig.9. Spleen of (MD) showing infiltration with large vesicular nuclei and abundant cytoplasm with lymphoid depletion (arrow), HEX50.

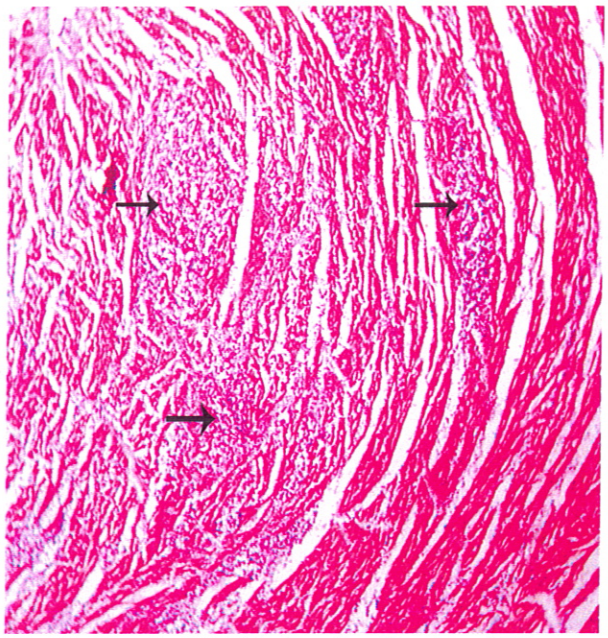

Fig.10. Heart of (MD) showing focal or diffuse infiltration of myocardium by pleomorphic cell aggregates (arrow), HEX100.

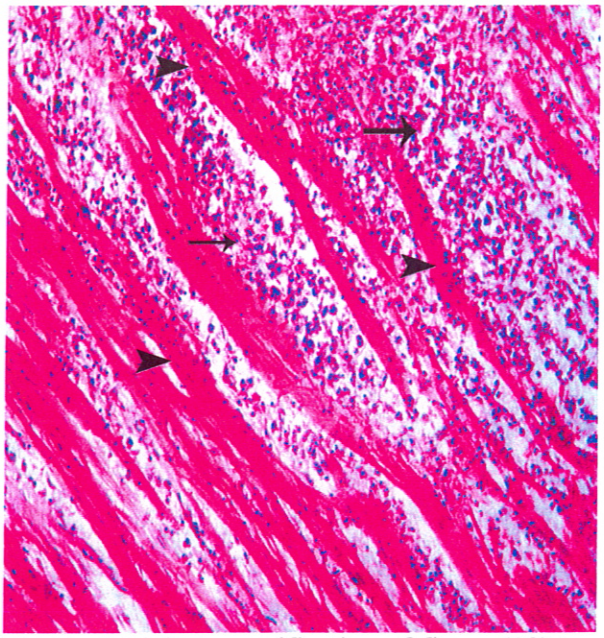

Fig.11. A higher magnification of figure (10) to show numerous pleomorphic cells (small, large lymphocytes, plasma cells and a few heterophils) infiltrating necrotic muscle fiber (arrow head), HEX400.

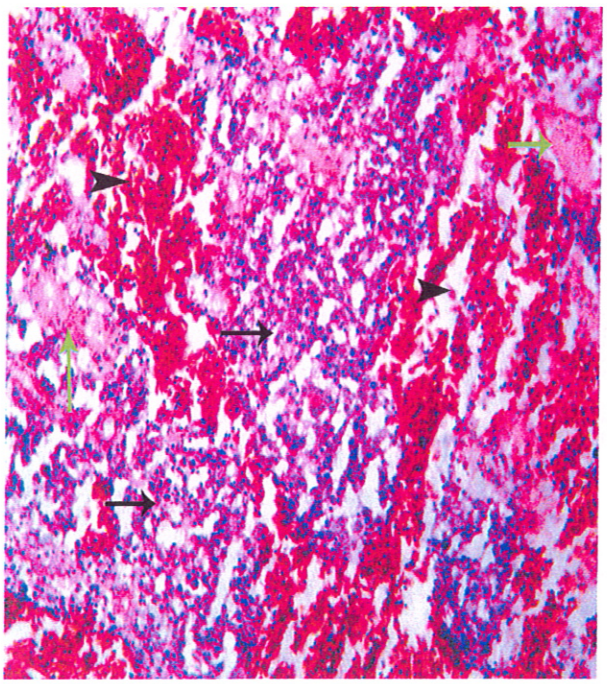

Fig.12. Kidney of (MD) showing aggregation of pleomorphic cells between necrotic renal tubules represented by pyknosis, karyorrhexis and karyolysis (green arrow) with hemorrhage (arrow head), HEX400.

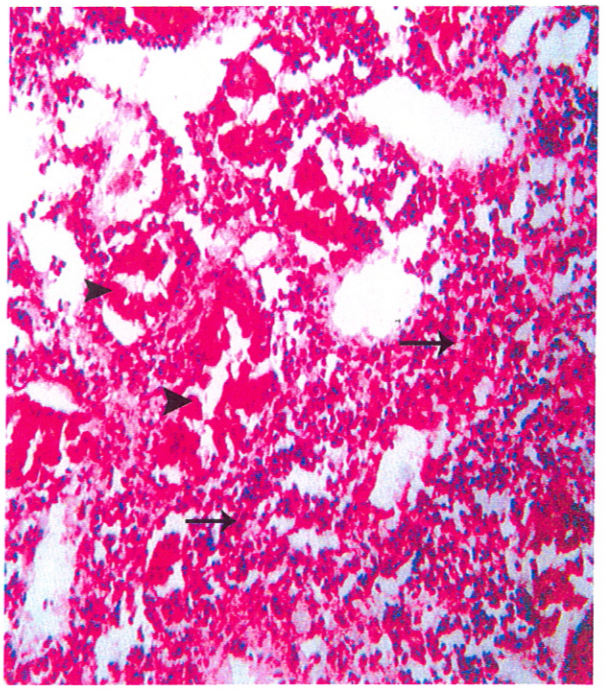

Fig.13. Kidney of (MD) showing necrotic renal tubules (arrow head) with replacement renal parenchyma by mature lymphocytes, lymphoblasts, plasma cell and heterophil cells (arrow), HEX400.

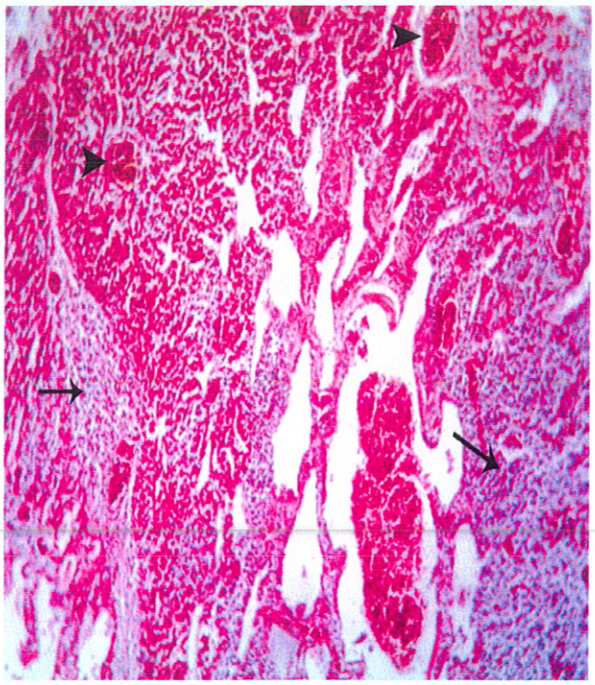

Fig.14. Lung of (MD) showing pleomorphic cells infiltrations particularly in the connective tissue septa (arrow) and around the blood vessels (arrow head), HEX50.

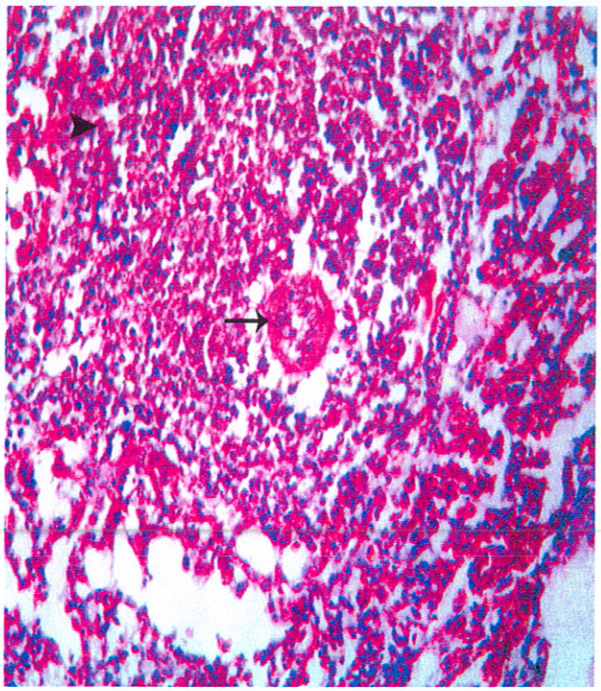

Fig.15. Lung of (MD) showing perivascular mature lymphocytes, lymphoblasts and plasma cells aggregations proliferation (arrow), HEX400.

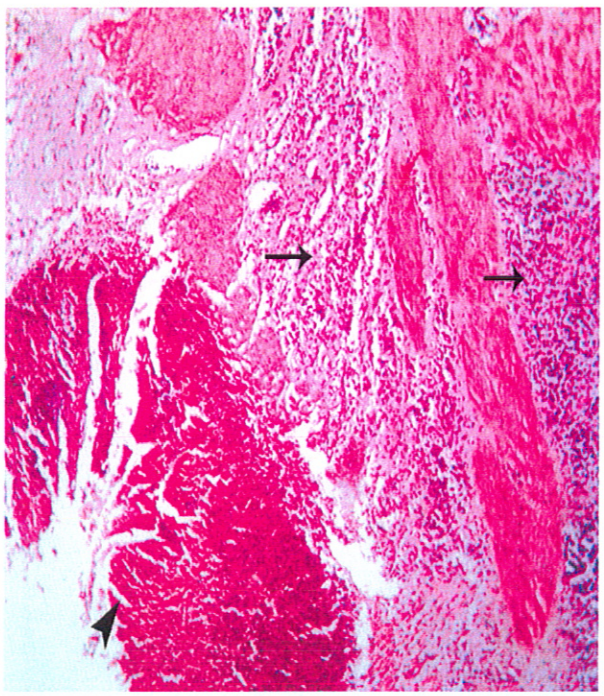

Fig.16. Proventriculus of (MD) showing invasion of the mucosa, muscularis mucosa by pleomorphic infiltration of lymphocyte, lymphoblast and heterophil cells (arrow) with mucosal necrosis (arrow head), HEX100.

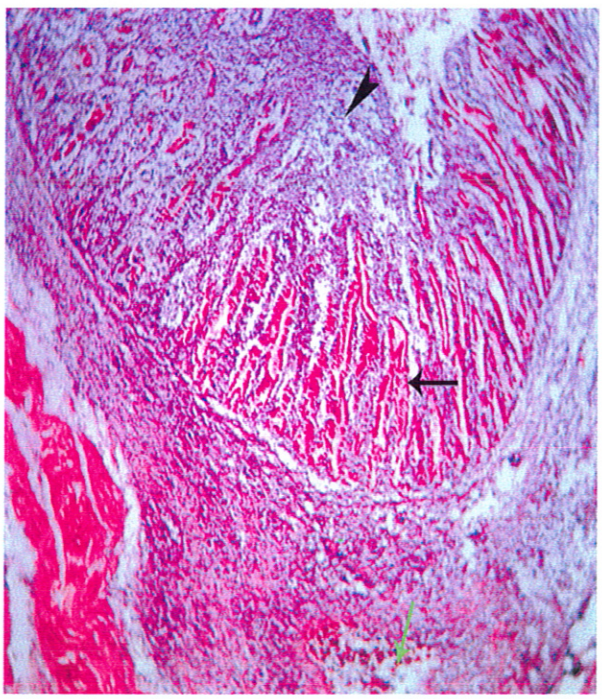

Fig.17. Proventriculus of (MD) showing mucosal infiltration by intense aggregations from pleomorphic cells (arrow head) and glandular necroses (arrow) and congestion of sub mucosal blood vessels (green arrow), HEX100.

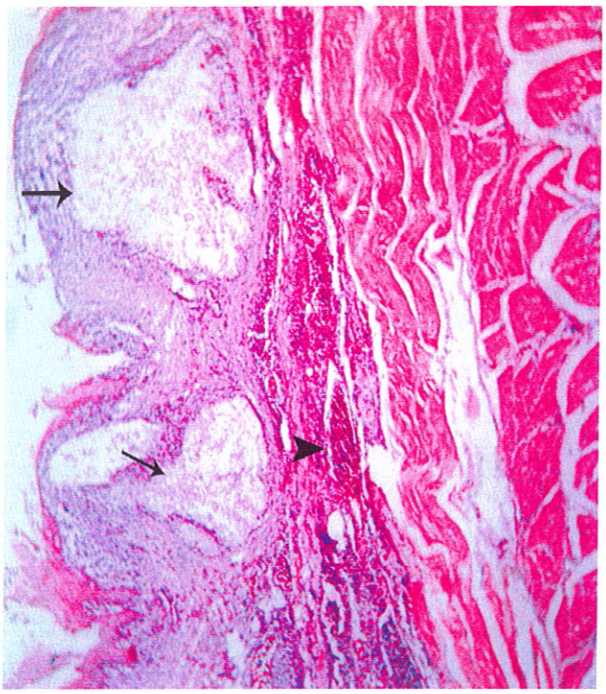

Fig.18. Gizzard of (MD) showing pleomorphic cells infiltrations around the small blood vessels in the submucosa, muscle layers (arrow head) and mucosal necrosis (arrow), HEX100.

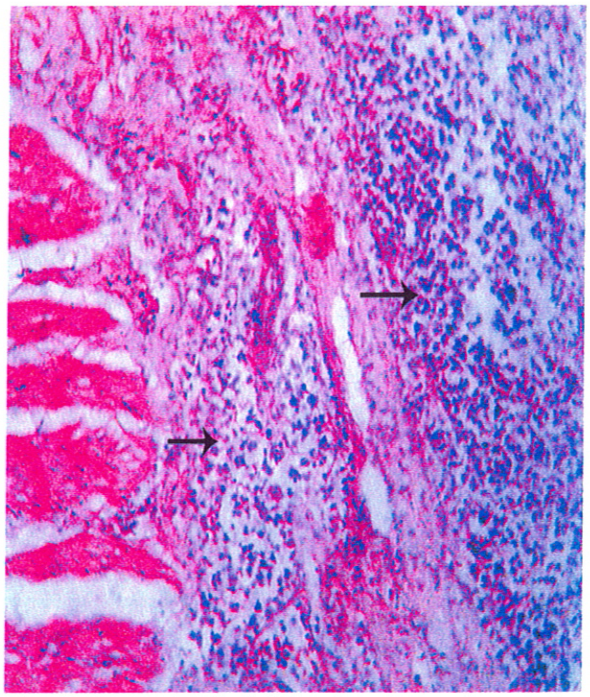

Fig.19.Gizzard of (MD) showing subserosal massive infiltrations from pleomorphic cells (arrow), HEX400.

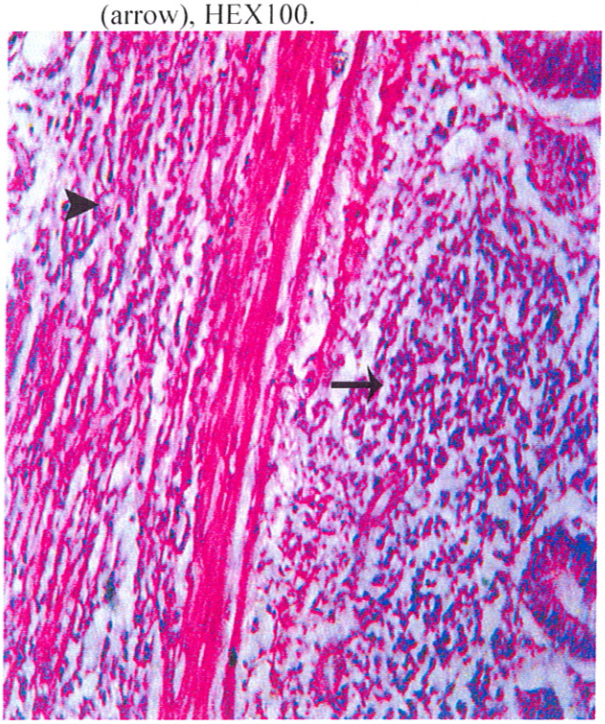

Fig.20. Intestine of (MD) showing replacement of mucosal layer (arrow) and submucosa (arrow head) with pleomorphic cells aggregations of with thickening of the intestinal wall (green arrow), HEX100.

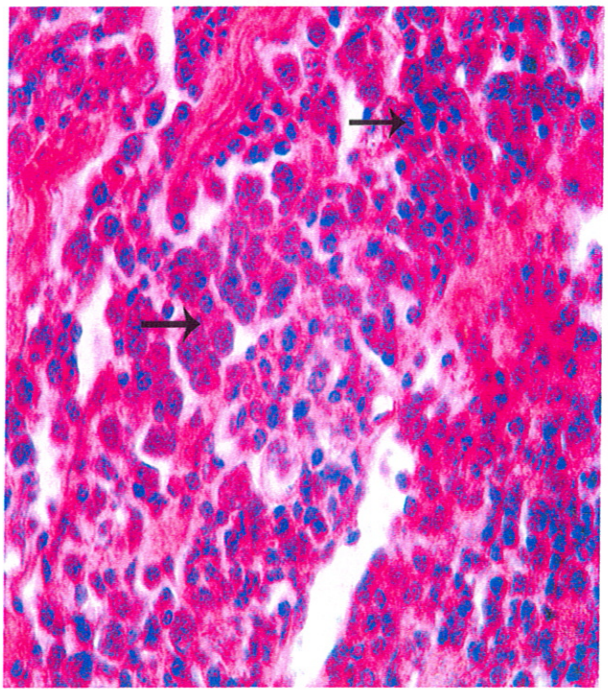

Fig.21. A higher magnification of fig (20) showing pleomorphic cells with large vesicular hyperchromatic nuclei and abundant esinophilic cytoplasm with clusters formation (arrow), HEX1000.

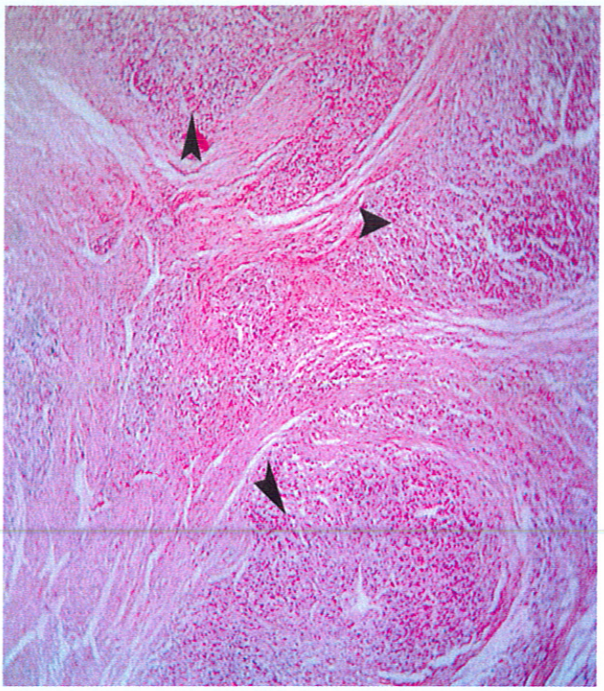

Fig.22. Bursa of Fabricius of (MD) showing inter follicular infiltration with pleomorphic cells aggregations (arrow head), HEX50.

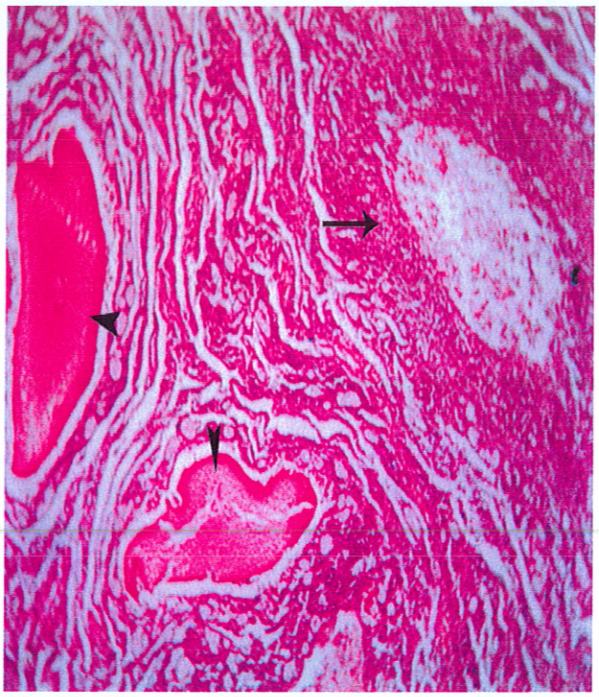

Fig.23. Ovary of (MD) showing degenerated or misshaped ova (arrow head) with intense lymphoid cell infiltration (arrow), HEX100.

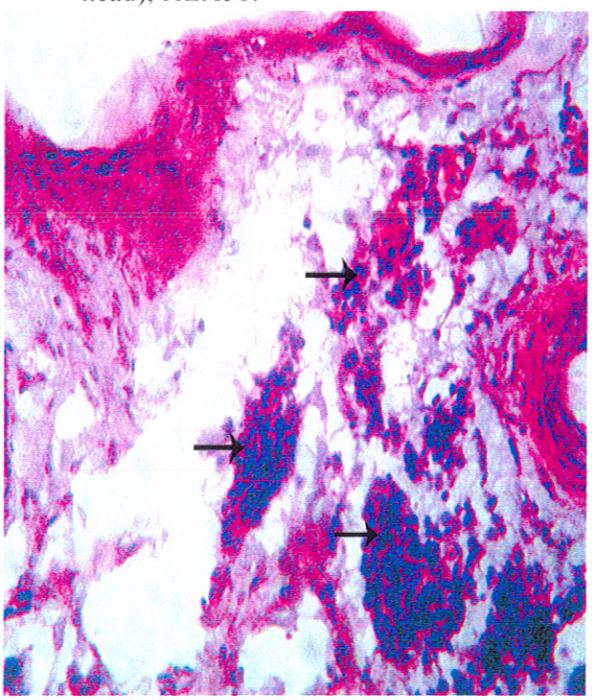

Fig.24. Skin of (MD) showing lymphoid cells aggregates in the dermis particularly around the dermal blood (arrow), HEX400.

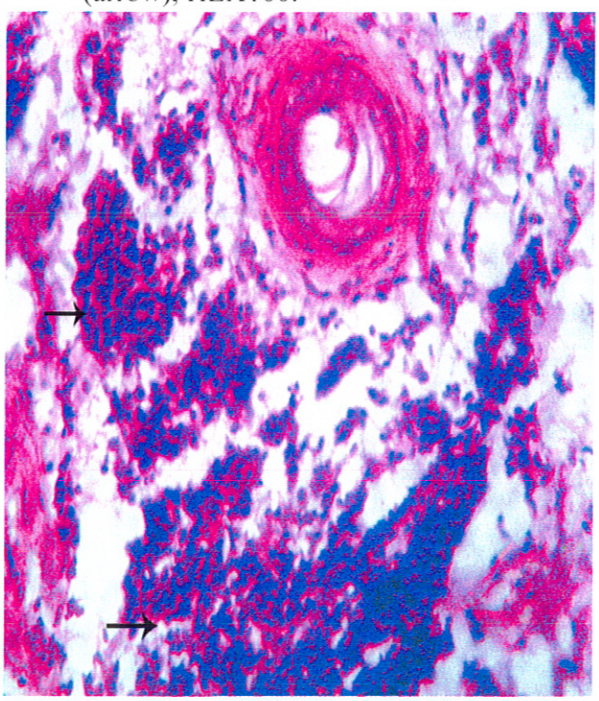

Fig.25. A higher magnification of fig (24) showing perivascular aggregation of lymphoid cells around dermal blood vessel (arrow), HEX400.

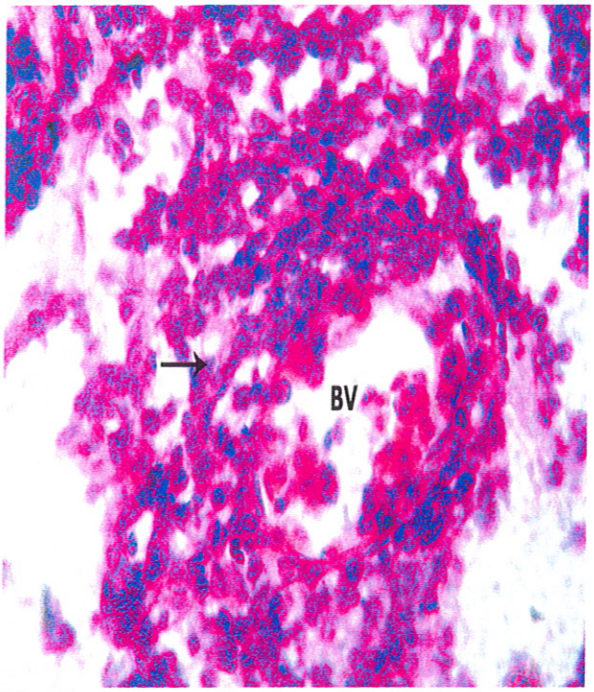

Fig.26. Oil magnification of fig (25) showing perivascular aggregation of pleomorphic cells with large oval vesicular hyper chromatic nuclei and scanty cytoplasm (arrow), HEX1000.

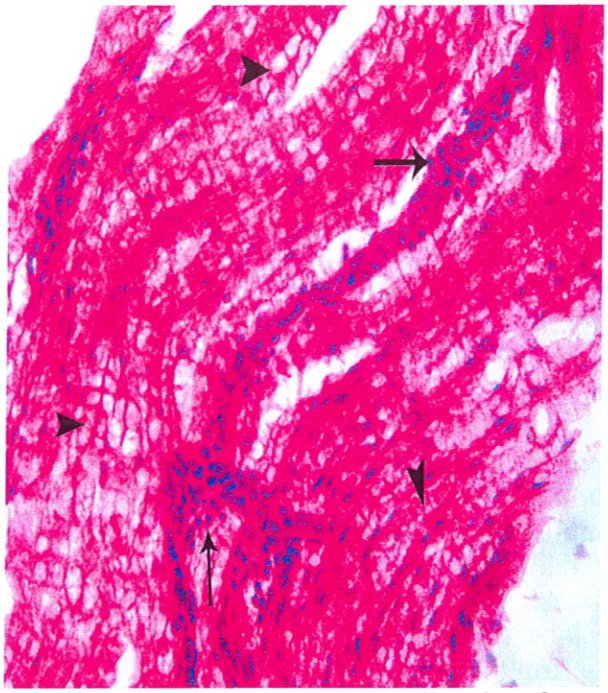

Fig.27. sciatic nerve of (MD) showing few pleomorphic cellular infiltrations (arrow) with focal thickened and demyelination (arrow head), HEX400.

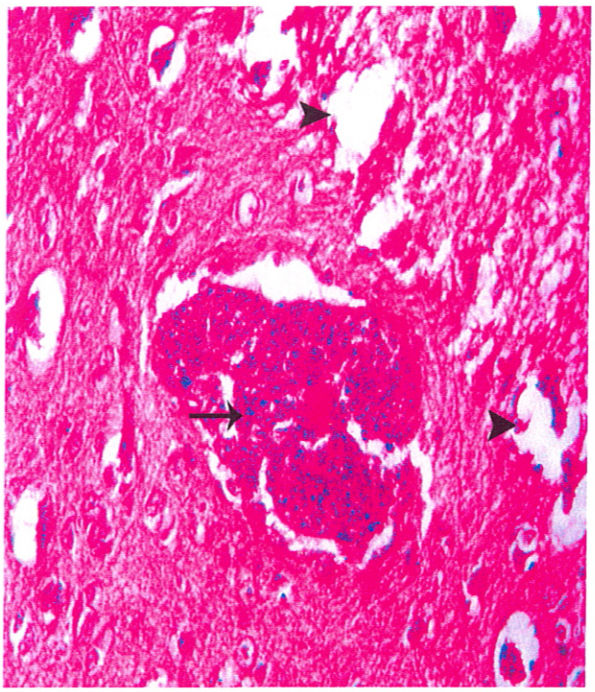

Fig.28. Brain of (MD) showing cytogenic edema represented by vacuolated neurons and neuronoglias (arrow head), HEX400.

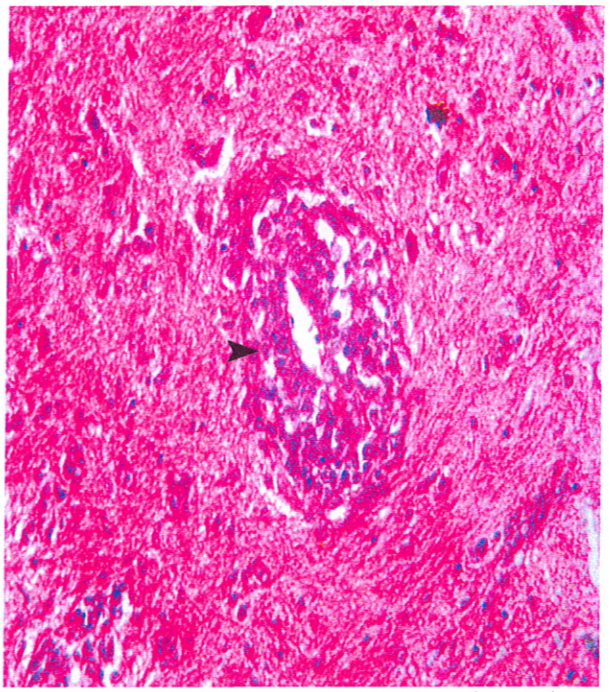

Fig.29. Brain of (MD) showing perivascular pleomorphic aggregation of T lymphocyte, lymphoblast, macrophage, plasma cells and heterophil cells (arrow head), HEX400.

DISSCUSION

In the past, molecular techniques such as PCR were developed for the diagnosis of MDV by DNA extracted from feather tips, lymphocytes or tissue samples from the infected chickens with the advantage that it could be used for both detection and differentiation between virulent and vaccine MDV strains *(20-22)*. PCR assays usually take several hours to complete including electrophoresis time making it time consuming diagnostic method, a technique that requires a well-established laboratory, a thermal cycler and a gel system to visualize respective amplified products. The most important aspect of the present study was to diagnose Marek's disease by the gross and histopathological lesions (simple and a more rapid way) and confirm the diagnosis by PCR *(23)*.

Ninety-seven out of 125 (77.6%) examined tissues specimens were diagnosed as Marek's disease. The pathological changes of Marek's disease have been reported by many authors, since the disease was first described by Marek in 1907.

Nervous disorders were the main clinical signs besides gasping, weakness, depression, in appetence, change in weight, diarrhea, immunosupression, emaciation and increased percentage of mortality. These results are in agreement with *(24- 26)*.

Macroscopically, enlargement of sciatic nerves, irregular pupil, grayish-white nodules in the visceral organs and focal discolored areas on the skin were noticed. The aforementioned lesions were similar to those described by *(26,27)* and partially similar to *(28)* who described that the gross lesion of Marek's in the classical form is enlargement of one or more of the peripheral nerves especially the brachial and sciatic plexus and nerve trunks, celiac plexus, abdominal vagus and intercostal nerves.

Microscopically, heavy pleomorphic cellular infiltrations of small lymphocytes, lymphoblasts, heterophils, plasma cells, fibroblasts and few mesenchymal cells were seen in all examined organs beside cellular mitosis. Extensive tissue necrosis, congestion, hemorrhage and edema were associated the infiltrations. A forementioned findings were in agreement with *(29- 32)*.

The bursa of Fabricius showed sharply demarcated lymphoid follicles with necrosis in the lymphoid cells at the center of the follicles. Sometimes, fibrous connective tissue proliferation was the cause of such demarcation. The tumor cells were seen in the interfollicular zones and rarely extended to the adjacent lymphoid follicles. Similar results were reported by *(33, 34)* and partially agreed with *(31)* who observed atrophied lymphoid follicles of bursa.

Necrosis in different cases is due to immunosuppression with inducing autoimmune disease where the T cell attacks the self cellular system. Similar finding were observed by *(35)*.

All investigated birds were regarded as one disease entity with lesions possessing the same characteristics, but of varying severity (by histopathology). PCR was best tool to detect and differentiate the Marek's disease virus; but consuming time.

It could be concluded that the prevalence of Marek's disease was high in different poultry flocks and it diagnosed by histopathology and other molecular investigations such as PCR.

REFERENCES

1.Fatunmbi OO and Adene DF (1986): A ten year prevalence study of Marek's disease and .avian leukosis at ibadan, nigeria acta VET. BRNO. Vol.55: 49-53.

2.Hirai K ed (2001): Current Topics in Microbiology and Immunology: Marek's Disease (Current Topics in Microbiology and Immunology). Springer: Berlin. ISBN Vol. 3:540-677.

3.Gilka F and Spencer JL (1993): Cytopathology caused by the AC-1 isolate of Marek's disease virus in the feather folloicle epidermis. Avian Pathol. Vol. 22:283-293.

4.Landman W. JM and Verschuren S. BE (2003): Titration of Marek's disease cell-associated vaccine virus (CVI 988) of reconstituted vaccine and vaccine ampoules from Dutch hatcheries'. Avian Dis. Vol.47:1458-1465.

5.Payne LN and Venugopal K (2000): Neoplastic diseases: Marek's disease, Avian leukosis and reticuloendotheliosis. Rev. Sci. tech.int, Epiz.Vol.19 (2):544-564.

6.Calnek BW, Aldinger HK, and Kahn DE (1970): Feather follicle epithelium: a source of enveloped and infectious cell-free herpesvirus from Marek's disease. Avian Dis. Vol.14:219–233.

7.Rooney WF and Bickford AA (1979): Marek's disease in backyard chicken flocks. Extention veterinarian university of California.Daris.

8-Baigent SJ, Smith LP, Nair VK, Currie RJW (2006): Vaccinal control of Marek'sdisease: current challenges, and future strategies to maximize protection. Veterinary Immunology and Immunopathology.vol.112:78-86.

9.Morrow C and Fehler F (2004): Marek's disease: a worldwide problem. Marek's disease: an Evolving Problem Elsevier Academic Press.

10.Nair V, Kung HJ (2004): Marek's disease virus oncogenicity: molecular mechanisms. Marek's Disease: an Evolving Problem Elsevier Academic Press.

11.Osterrieder N, Kamil JP, Schumacher D, Tischer BK, Trapp S(2006): Marek's disease virus: from miasma to model. Nature Reviews Microbiology 2006, 4:753-761.

*12. Shambhu DS, Rajamani B, Asok K, Rajib D, Amit KV and Kuldeep D (2012):*Recent Trends In Diagnosis and Control of Marek's Disease (MD) in poultry. Pakistan Journl of Biological Sciences.Vol.15 (20):964-970.

13.Davidson. I (2009): The knowledge that human tumor virology can gain from studies on avian tumor viruses. Adv. Tumor Virol.Vol. 1: 9 –19.

14.Suvarna SK, Layton C and Bancroft JD (2013): Bancroft's Theory and Practice of Histological Techniques. 7th ed., Churchill Livingstone. Elsevier, England.

15. Sambrook J, Fritscgh EF and Mentiates T (1989): Molecular coloning. A laboratory manual. Vol. 1 Cold spring Harbor Laboratotry press, New York.

16. Handberg, KJ, Nielsen OL and Jørgensen PH (2001): The use of serotype 1- and serotype 3-specific polymerase chain reaction for the detection of Marek's disease virus in chickens. Avian Pathology vol. 30: 243– 249.

17.OIE (2009): **Office International des-Epizooties** (Marek's disease. In: Manual of Standards for Diagnostic Tests and Vaccines. OIE Terrestrial Manual. 5th Edn., Rome.

18.Mitra N, Verma R and Singh A (2013): Early Detection of Avian Oncogenic Viruses from Blood of Apparently Healthy Chickens. Proceedings of the National Academy of Sciences, India Section B: Biological Sciences. vol. 83: 53-58.

19. Wei K, Sun Z, Zhu S, Guo w, Sheng, P, Wang Z, Zhao C, Zhao Q and Zhu R (2012): Probable Congenital Transmission of Reticuloendotheliosis Virus Caused by Vaccination with Contaminated Vaccines. PLoS ONE Vol. 7 (8).

20.Baigent SJ, Smith LP, Currie RJ, Nair V (2005): Replication kinetics of Marek's disease vaccine virus in feathers and lymphoid tissues using PCR and virus isolation, J Gen V. 86, 2989-2998.

21.Becker Y, Asher Y, Tabor E, Davidson I, Malkinson M and Weisman Y(1992):

Polymerase chain reaction for differentiation between pathogenic and non-pathogenic serotype 1 Marek's disease viruses (MDV) and vaccine viruses of MDV-serotypes 2 and 3 V. 40.

22.Krol K, Samorek-Salamonowicz E, Kozdrun W, and Wozniakowski G(2007): Duplex PCR assay for detection and differentiation of pathogenic and vaccine strains serotype 1, Bull Vet Inst Pulawy,Vol. 51: 331-335.

23.Notomi T, Okayama H, Masubuchi T, Yonekawa T, Watanabe K, Amino N and Hase T(2000): Loop-mediated isothermal amplification of DNA, Nucleic Acids Res., 28(12): 63.

24.Yutaka F, Michio NA, Kosuke O, Masaaki O and Kiyoshi MWA (1971): Pathological Studies of Marek's Disease. The Histopathology on Field Cases in Japan. Jap. J. Vet. Res. Vol. 19:7-26.

25.Rooney WF and Bickford AA (1979): Marek's disease in backyard chicken flocks. Extention veterinarian university of California.Daris.

26. Ekperigin HE, Fadly AM, Lee LF, Liu X and Mccapes RH (1983): Comb lesions and Mortality Patterns in white Leghorn Layers affected by Marek's disease. Avian Diseases, Vol.27 (2):503-512.

27.OIE (2004): Office International des-Epizooties (Marek's disease. In: Manual of Standards for Diagnostic Tests and Vaccines. OIE Terrestrial Manual. 5th Edn., Rome.

28.Payne LN and Venugopal K (2000): Neoplastic diseases: Marek's disease, Avian leukosis and reticuloendotheliosis. Rev. Sci. tech.int, Epiz.Vol.19 (2):544-564.

29.Ionica F, Coman M and Catana N (2009): An out break of Marek's disease in Broiler chickens: Epidemiological, clinical and Anatomopathological Aspects. Lucrari stiintifice medicina veterinara . Vol.xlii(1):224-227.

30.Hikmet K, Fatih FA, Hakki CI, Ismail K, Erkan K and Yilmaz D (2010): Increased DNA damage and oxidative stress in chickens with Natural Marek's Disease. Veterinary Immunology and Immunopathology 133: 51–58.

31.Hablolvarid MH(2011):Investigation on Incidence of Marek's Disease in Broiler Flocks of some Regions in Tehran Province, Iran Archives of Razi Institute, Vol. 66(2):109-114.

32.Sathish G, Parthiban M, Kumanan K, Balachandran C and Kurunchi CD (2012): Differential Detection of Avian Oncogenic by Use of Multiplex PCR Viruses in Poultry Layer Farms and Turkeys J. Clin. Microbial. Vol.50 (8):2668-2673.

33.Frank JS and Burmester BR (1970): The differential diagnosis of lymphoid leukosis and Marek's disease. Regional Poultry Research.

34.Payne LN and Rennie M (1976): The proportions of B and T lymphocytes in lymphomas, peripheral nervesand lymphoid organs in Marek's disease. Avian Pathol. Vol. 5:147-154.

35.Amerio P, Toto P, Feliciani C,Suzuki H, Shivji G, Wang B and Sauder N(2002): Rethinking the role of tumour necrosis factor in ultraviolet (UV) b-induced immunosuppression:altered immune response in UV-irradiated TNFRIR2 gene-targeted mutant mice.

الملخص العربى

دراسات تشخيصيه مقارنه على مرض ماريك في الدجاج باستخدام الفحص الهستوباثولوجى والفحص الجزيئي

عبدالمنعم احمد على ، السيد رشاد العطار، محمد حامد محمد ،هبه محمد عبد الغنى
قسم الباثولوجيا- كليه الطب البيطرى- جامعه الزقازيق

هذه الدراسه تعطى الضوء على اهم الاورام السرطانيه فى الدواجن واهمها مرض الماريك ومعرفه مدى انتشار الفيروس بين قطعان الدجاج في المناطق المختلفة على أساس التفتيش الدقيق لجثث الدجاج في مختلف المزارع وباستخدام الفحص الباثولوجى واختبار البى سى ار.

لقد تم جمع مائه خمسه وثلاثون طائر من مختلف أسراب الطيور الداجنة و حالات متفرقة بين الفترة من أغسطس ١٥، ٢٠١٢ إلى نوفمبر ٨، ٢٠١٤ وقد قد تم نجميع عينات من الكبد والطحال والقلب والرئتين والكلى و الأمعاء والمبيض، الأحشاء والجلد و الأعصاب، والعين والدماغ من كل حالة وتعرضوا للفحص الباثولوجى واختار منها 7حالات مخزنه عند -٢٠ لفحص البى سى ار.

وكانت اهم الاعراض الظاهره على هذه الطيور اضطرابات عصبيه فى الرقبه والاجنحه والساقين و صعر وتدلى من الاجنحه وشلل فى الساقين او الاجنحه فى جانب واحد او كلا الجانبين وتقويس داخلى لاصابع القدم واسهال و هزال إلى جانب ما يصل إلى ١٥ ٪ وفيات.

اما اهم الافات الظاهره على هذه الطيوركانت زياده فى سمك الاعصاب الوركيه وعم انتظام بؤبؤ العين وقد لوحظت عقيدات رماديه بيضاء في الأجهزة الحشوية وتغيرات بؤريه فى لون الجلد الى جانب احتقان المبايض وتشوه البويضات.

ولقد كانت اهم الافات المجهرية هى وجود اشكال متعددة من الخلايا الليمفاويه الصغيره والابيضاض الليمفاوى وخلايا البلازما وقليل من خلايا اللحمه المتوسطه فى معظم العينات المفحوصه الى جانب تنخر واسع النطاق فى الأنسجة ، واحتقان و نزف ووذمه. وكان ستة حالات من أصل سبعة تعرضوا لاختبار بى سى ار إيجابي لفيروس مرض ماريك.

ولقد لوحظ ان جميع الطيور ظهر عليها نفس الاعراض ونفس الافات المجهريه ولكنها تختلف فى شدتها وكان البى سى ار أفضل وسيلة لاكتشاف و تمييز فيروس مرض ماريك . لكن تستغرق وقتا طويلا.